

Performance Comparison of Using SOA and HNLf as FWM Medium in a Wavelength Multicasting Scheme with Reduced Polarization Sensitivity

Dawei Wang, *Student Member, IEEE*, Tee-Hiang Cheng, *Senior Member, IEEE*, Yong-Kee Yeo, *Member, IEEE*, Zhaowen Xu, Yixin Wang, Gaoxi Xiao, *Member, IEEE*, and Jianguo Liu

Abstract—In this paper, we propose and demonstrate the practical all-optical wavelength multicasting scheme based on the four-wave mixing (FWM) effect in both a highly nonlinear fiber (HNLf) and a semiconductor optical amplifier (SOA). Then we carry out comprehensive comparisons of the performance differences between using the HNLf and SOA for this proposed multicasting scheme. Seven multicast channels are experimentally demonstrated by using three co-polarized probes and a modulated signal. The merit of the proposed scheme is that the polarization sensitivity is significantly reduced from more than 20 dB to approximately 5 dB using the HNLf and 2.5 dB using the SOA. The low polarization sensitivity leads to a difference of less than 1 dB in the power penalty of the multicast channels at bit error rate (BER) = 10^{-9} . In addition, we compare the multicasting performance of the on-off keying (OOK) and differential phase-shift keying (DPSK) signals using the proposed scheme and found that the power penalties of the DPSK multicast channels in the HNLf and the SOA are less than 1.25 dB and 1.1 dB respectively, and the power penalties of the OOK multicast channels are less than 1.5 dB and 3.1 dB in the HNLf and the SOA respectively.

Index Terms—Optical wavelength multicasting, four-wave mixing, fiber optics communications, polarization sensitivity, all optical network

I. INTRODUCTION

All-optical packet switching (OPS) is a promising technology for future optical network as it can fully utilize the network bandwidth with its packet level switching granularity [1]. In addition, it eliminates the expensive optical-electronic-optical (O/E/O) conversions of payload in intermediate nodes [2]. Nevertheless, a large number of network and physical layer design issues need to be addressed before OPS can be realized [1]-[24]. These issues include

packet contention resolution, multicasting, optical label processing, optical switch fabric design, optical buffering, optical wavelength conversion, all-optical 2R/3R signal regeneration, burst-mode transmitter/receiver, burst mode-amplifier, and clock recovery.

Multicasting, where information can be replicated to multiple selected destinations, is one of the desirable features of OPS. By means of multicasting, the efficiency and throughput of high-speed wavelength division multiplex (WDM) optical networks can be improved significantly in the presence of multicast traffic. Multicasting can be implemented in the network or physical layers [7], [10], [11], [25]-[40]. In this paper, we focus on physical layer multicasting.

Substantial effort has been made to realize all-optical wavelength multicasting [25]-[32]. These techniques can be classified into cross-gain modulation (XGM), cross-phase modulation (XPM), self-phase modulation (SPM), cross-absorption modulation (XAM), and fiber-optics parametric amplifier (FOPA) in the fibers with high nonlinearity, electro-absorption modulator (EAM), or semiconductor optical amplifier (SOA). However, these techniques are applicable to only the on-off keying (OOK) signal format. Since a modern optical communications system should have the flexibility to support different modulation signal formats [41], [42], a multicasting technique that is modulation-format and bit-rate transparent is highly desirable. To achieve such transparency, several multicasting schemes based on multi-pumps induced four-wave mixing (FWM) effect have been proposed [33]-[40].

To implement a multi-pump FWM based multicasting scheme in a real system, an important practical issue that needs to be addressed is polarization sensitivity [33]-[40]. In our previous work [35], we have demonstrated an all-optical wavelength multicasting technique in a highly nonlinear fiber (HNLf)-based Sagnac loop mirror, which overcomes the undesirable effect of pump-pump generated idlers overlapping with the multicast channels. However, the polarization states of the pumps and signal need to be adjusted to obtain the best conversion efficiency (CE) for all the multicast channels. As the state of polarization (SOP) of the input data signal is random in general, this requires the SOPs of the pumps to be

Manuscript received in June 20, 2010. This work was supported by an A*STAR SERC Grant (Award No. 0721010019).

D. Wang, T.-H. Cheng, and G. Xiao are with the School of Electrical and Electronic Engineering, Nanyang Technological University, Singapore 639798 (e-mail: wang0365@ntu.edu.sg, Ethcheng@ntu.edu.sg, Egxxiao@ntu.edu.sg)

Y.-K. Yeo, Z. Xu, and Y. Wang are with the Institute for Infocomm Research, 1 Fusionopolis Way, Singapore 138632 (e-mail: ykyeo@i2r.a-star.edu.sg, zxu@i2r.a-star.edu.sg, wangyx@i2r.a-star.edu.sg).

J. Liu is with Institute of Semiconductors, Chinese Academy of Sciences, China (e-mail: jgliu@semi.ac.cn).

adjusted from time to time to achieve the highest CE for all the multicast channels. Otherwise, the CE fluctuation of the multicast channels due to the polarization sensitivity is more than 20 dB [43]-[48]. This may not be practical for a real system.

Lots of schemes for realizing the FWM based low polarization sensitive wavelength conversion have been reported [43]-[48]. However, regarding to the FWM based low polarization sensitive wavelength multicasting, not so much work is reported [39], [40], which is due to the operation complexity. In [39], the authors proposed a polarization insensitive wavelength multicasting scheme based on FWM in a photonic crystal fiber (PCF) with residual birefringence. In that scheme, one optical pump needs to be coupled into the PCF precisely at 45 degree to the principal axes. In addition, only five error-free multicast channels, including the signal itself, are generated by using three-pump laser sources. In another of our previous work [40], we proposed and demonstrated a practical all-optical wavelength multicasting scheme based on the FWM effect in an HNLf with reduced polarization sensitivity. By using three co-polarized probes with pre-defined wavelength separations, three beating gratings are generated to scatter the modulated signal to be far away from the probes to avoid unwanted crosstalk [43], [44]. This way, six new multicast channels, which have rather small polarization dependence on the modulated signal, are generated. Thus, seven multicast channels, including the signal itself, are obtained at the output of HNLf. Comparing with the requirement of precisely coupling condition in [39], another advantage of our proposed scheme is that the co-polarized probes are easily obtained by using the polarization maintaining devices at the output of laser sources.

However, in [40], only OOK signal is demonstrated for multicasting performance in the HNLf. In this paper, we demonstrate both OOK and differential phase-shift keying (DPSK) signals multicasting using an HNLf and an SOA. Although both HNLf and SOA have been reported for low polarization sensitive wavelength conversion, their applications to low polarization sensitive wavelength multicasting were not reported in the previous study. In addition, we comprehensively compare the performance differences of using these two nonlinear mediums to perform our proposed wavelength multicasting scheme. Experimental results show that the power fluctuations of the converted multicast channels due to the polarization sensitivity are greatly reduced from more than 20 dB [43]-[48] to about 5 dB in an HNLf and 2.5 dB in an SOA. The maximum power penalties (at bit error rate (BER) = 10^{-9}) of the OOK and DPSK multicast channels are less than 1.5 dB and 1.25 dB in the HNLf respectively, and less than 3.1 dB and 1.1 dB in the SOA respectively. Furthermore, the power fluctuations of the multicast channels due to the residual polarization sensitivity only leads to less than 1 dB power penalty differences.

The rest of this paper is organized as follows. Section II explains the operation principle of the proposed polarization sensitive reduced optical wavelength multicasting scheme. The experimental setup, results, and performance comparison

discussions are reported in Section III. Finally, the paper is concluded in Section IV.

II. OPERATION PRINCIPLE

Both HNLf and SOA can be used as the nonlinear medium to perform the FWM effect based optical wavelength multicasting. The advantages and disadvantages of employing HNLf and SOA for nonlinear optical applications are summarized in Table I. The performance comparison pertaining to their applications to our proposed low polarization sensitivity wavelength multicasting scheme is reported in Section III.

TABLE I
Advantages and disadvantages of using HNLf and SOA for nonlinear optical applications

	Advantages	Disadvantages
HNLf	(a). Ultrafast response time (b). Low noise figure (c). Passive device (no power consumption) (d). Wide and flat band wavelength conversion bandwidth	(a). Low conversion efficiency (b). Difficult for photonics integration
SOA	(a). Easy for photonics integration (b). Compact in size (c). High conversion efficiency	(a). Limited carrier recovery time (b). Large amplifier spontaneous emission (ASE) noise figure (c). Active device (power consumption)

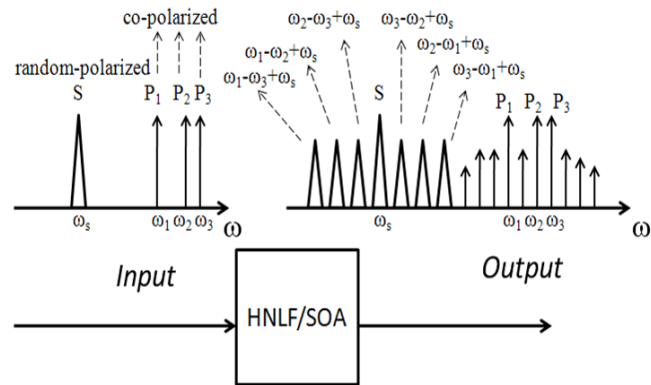


Fig. 1. Operation principle of this proposed polarization sensitivity reduced multicasting technique.

Fig. 1 illustrates the operation principle of this proposed polarization sensitive reduced multicasting technique. The signal (S) with electrical field (E_s) is coupled into the HNLf/SOA with random polarization. Three probes (P_1 - P_3) with electrical fields (E_1 - E_3) are co-polarized with each other and coupled into the HNLf/SOA. Their frequency separations are pre-defined, e.g., 100-GHz between P_2 and P_3 , 200-GHz between P_1 and P_2 , and 300-GHz between P_1 and P_3 . From Fig. 1, it can be seen that six FWM generated multicast channels are located at both sides of the signal symmetrically. In addition, other FWM produced idlers also appear at the output of the HNLf/SOA. In order to make the multicast channels separate

from the other FWM idlers, we set the frequency of the signal far away from the probes.

We will first describe the operation principle of this proposed multicasting scheme in the HNLf. Take the multicast channel at the frequency of $\omega_1 - \omega_2 + \omega_s$ as example, which is composed of two FWM idlers. Co-polarized probes P_1 and P_2 generate a beating grating, and then this beating grating scatters the modulated signal. Consequently two new FWM idlers are generated on both sides of the signal symmetrically, with the frequencies of $\omega_1 - \omega_2 + \omega_s$, and $\omega_2 - \omega_1 + \omega_s$ respectively. These two idlers have constant powers with respect to any SOP of the signal [43].

On the other hand, S and P_2 also generate a beating grating. This beating grating then scatters P_1 to generate two idlers at the frequencies of $\omega_s - \omega_2 + \omega_1$, and $\omega_2 - \omega_s + \omega_1$. The power of these two idlers however strongly depends on the SOP of the signal. The power of the idlers reaches maximum value when the signal has the same polarization as the probes, and becomes zero when the SOP of the signal is orthogonal to that of the probes.

Based on the above analysis, the electrical field of the multicast channel at the frequency of $\omega_1 - \omega_2 + \omega_s$ can be expressed by [44]

$$\begin{aligned} \vec{E}_i = & (\vec{E}_1 \cdot \vec{E}_2) r(\omega_1 - \omega_2) \vec{E}_s \cdot \exp j [(\omega_1 - \omega_2 + \omega_s)t + (\phi_1 - \phi_2 + \phi_s)] \\ & + (\vec{E}_s \cdot \vec{E}_2) r(\omega_s - \omega_2) \vec{E}_1 \cdot \exp j [(\omega_s - \omega_2 + \omega_1)t + (\phi_s - \phi_2 + \phi_1)]. \end{aligned} \quad (1)$$

Where $r(\omega_1 - \omega_2)$ and $r(\omega_s - \omega_2)$ denote the relative conversion efficiency functions, which decrease rapidly with the increase of the spacing between the two pumps [49]. For ease of discussion, the fiber loss is not taken into consideration.

As P_1 and P_2 are co-polarized with each other and θ represents the polarization angle between the signal and probes, the power of this channel can be expressed as [43]

$$P_i = \vec{E}_i \cdot \vec{E}_i^* = P_1 P_2 P_s [r^2(\omega_1 - \omega_2) + r^2(\omega_s - \omega_2) \cos^2 \theta]. \quad (2)$$

Since $r(\omega_s - \omega_2)$ is smaller than that of $r(\omega_1 - \omega_2)$, and also the power of the second component, which depends on the polarization angle θ between the signal and probes, can be treated as the small variation to this multicast channel. Therefore, the polarization sensitivity of the multicast channels is greatly reduced.

Then we replace the HNLf with an SOA in our proposed all-optical multicasting scheme and still take the multicast channel at the frequency of $\omega_1 - \omega_2 + \omega_s$ as example. Similar to that in the HNLf, this channel is also composed of two FWM idlers. Suppose the gain (G) of the SOA is polarization insensitive for simplicity, and we employ the lumped model to describe the FWM effect in the SOA [44]. Then the electrical field of this channel can be expressed as [44]

$$\begin{aligned} \vec{E}_i = & \sqrt{G_1 G_2 G_s} (\vec{E}_1 \cdot \vec{E}_2) r(\omega_1 - \omega_2) \vec{E}_s \cdot \exp j [(\omega_1 - \omega_2 + \omega_s)t + (\phi_1 - \phi_2 + \phi_s)] \\ & + \sqrt{G_1 G_2 G_s} (\vec{E}_s \cdot \vec{E}_2) r(\omega_s - \omega_2) \vec{E}_1 \cdot \exp j [(\omega_s - \omega_2 + \omega_1)t + (\phi_s - \phi_2 + \phi_1)]. \end{aligned} \quad (3)$$

where G_1 , G_2 and G_s mean the P_1 , P_2 , and S gain in the SOA, respectively. $r(\omega_1 - \omega_2)$ and $r(\omega_s - \omega_2)$ still represent the relative conversion efficiency functions in SOA and decrease rapidly with the increase of the spacing between the two pumps [50].

The power of this channel can be expressed as [44]

$$P_i = \vec{E}_i \cdot \vec{E}_i^* = G_1 G_2 G_s P_1 P_2 P_s [r^2(\omega_1 - \omega_2) + r^2(\omega_s - \omega_2) \cos^2 \theta]. \quad (4)$$

Since $r(\omega_s - \omega_2)$ is much smaller than $r(\omega_1 - \omega_2)$, the power of the second component, which also depends on the polarization angle θ , is treated as the variation to the overall power of this channel.

To summarize, the power of the multicast channels is almost polarization insensitive to the input signal. In the existing results [33]-[38], the CE of the multicast channels depends on the polarization angle between the signal and the pumps, similar to that observed in the second FWM idler in (2) and (4).

In addition, as the phases and amplitudes of the three probes are constant and do not carry any data information, it can be concluded from (1) and (3) that the phase and amplitude information of the signal can be preserved in all the multicast channels.

III. EXPERIMENTS AND RESULTS

A. Multicasting in HNLf

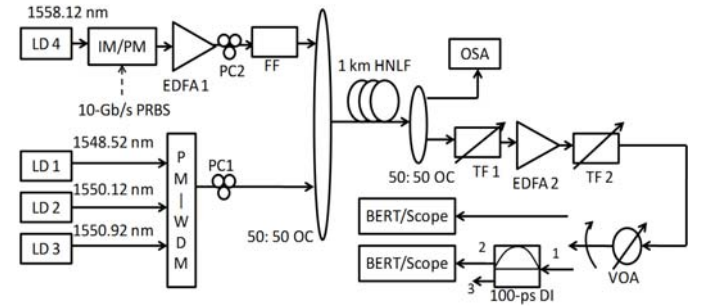


Fig. 2. Experimental setup. LD: laser diode. FF: fixed-wavelength filter. OSA: optical spectrum analyzer. IM: intensity modulator. PM: phase modulator. PC: polarization controller. HNLf: highly nonlinear fiber. OC: optical coupler. EDFA: erbium doped fiber amplifier. PRBS: pseudo-random bit sequence. PM-WDM: polarization maintaining wavelength division multiplexer. DI: delay interferometer. TF: tunable-wavelength filter. VOA: variable optical attenuator.

The experimental setup is shown in Fig. 2. Three laser diodes (LD1, LD2, and LD3 at 1548.52 nm, 1550.12 nm, and 1550.92 nm respectively) that are multiplexed by a polarization maintaining wavelength division multiplexer (PM-WDM) are used as the probes. Because the three probes have the same SOPs when they emit from the LD sources, the SOPs of the probes remain co-polarized with each other when they are introduced to the subsequent HNLf. Polarization controller (PC) 1 is used to adjust the overall SOP of the three co-polarized probes. LD4 (at 1558.12 nm) as modulated signal is intensity modulated (IM)/phase modulated (PM) by a 10-Gb/s $2^{31}-1$ pseudo-random bit sequence (PRBS) data and

then amplified by erbium doped fiber amplifier (EDFA) 1. A fixed-wavelength filter (FF) is used to reject the ASE noise. Different SOPs of the input modulated signal can be achieved by adjusting PC2.

The power of each probe that is coupled to the HNLf is set to about 3-dBm, and the power of the modulated (OOK and DPSK) signal is around 12-dBm. At the receiver side, tunable-wavelength filter (TL) 1 is used to select the desired multicast channel at the output of HNLf. EDFA2 is used to amplify this channel and TF2 is used to reject the ASE noise. Variable optical attenuator (VOA) is used to adjust the optical power before the eye diagram and BER of a multicast channel are measured. For receiving the 10-Gb/s DPSK modulated signal, a 100-ps delay interferometer (DI) is used to demodulate the DPSK signal.

The nonlinear coefficient of the HNLf is $11\text{W}^{-1}\text{Km}^{-1}$ and the zero dispersion wavelength λ_0 is 1560 nm. The dispersion slope and the total fiber loss at λ_0 are 0.035 ps/km-nm^2 and 2.3 dB respectively.

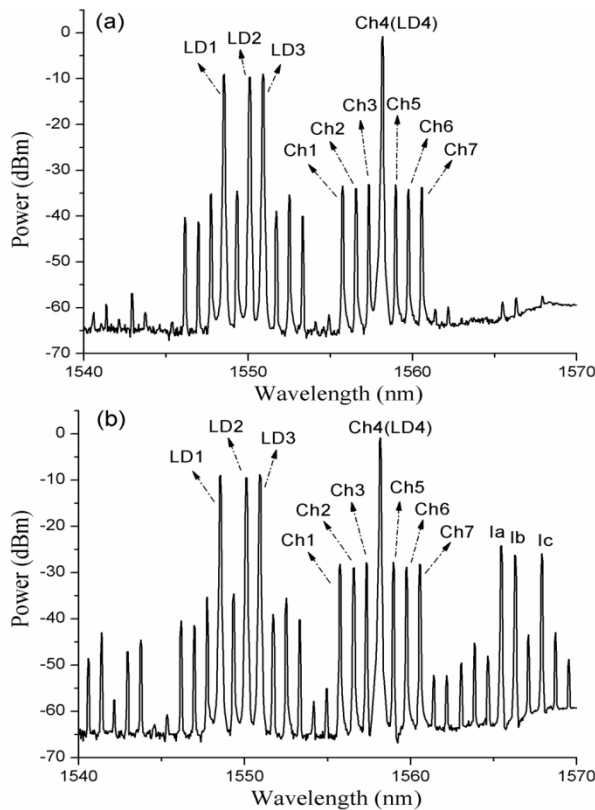


Fig. 3 (a) and (b). Optical spectra measured by the OSA when the OOK signal is orthogonal (a) and parallel (b) to the three co-polarized probes by using the HNLf.

Fig. 3 (a) and (b) show the optical spectra at the output of the HNLf when the SOP of the modulated OOK signal is orthogonal and parallel to the three co-polarized probes. Seven multicast channels, including the signal itself, with 100-GHz spacing are individually located at 1555.72 nm (Ch1), 1556.52 nm (Ch2), 1557.32 nm (Ch3), 1558.12 nm (Ch4), 1558.92 nm (Ch5), 1559.72 nm (Ch6), and 1560.52 nm (Ch7). As shown in Fig. 3, the difference in power level among the six FWM generated multicast channels is within 1 dB. The CE, defined as

the power of multicast channel over the power of output probe, is around -23.5 dB when the SOP of the signal is orthogonal to the probes; it increases to about -18.5 dB when the SOP of the signal is parallel to the probes. By varying the SOP of the input signal, the CE varies from -18.5 dB to -23.5 dB. Therefore, the polarization sensitivity is greatly reduced and this results in only about 5 dB conversion power fluctuation.

In addition, we can see from Fig. 3 that the CE fluctuation of Ia, Ib, and Ic is more than 30 dB when the SOP of the signal is varied. This provides additional evidence that the FWM CE greatly depends on the polarization states between the signal and pumps if no special techniques are used to reduce the polarization sensitivity. It is found that the number of other higher order FWM products in Fig. 3 (a) is obviously much less than that in Fig. 3 (b). This is because extra beating gratings will be generated among the signal and probes as the SOP of the modulated signal is parallel to the probes.

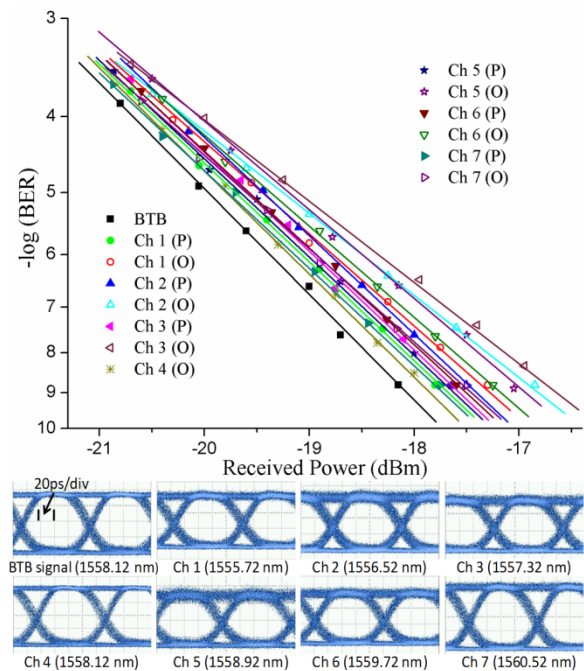


Fig. 4. BER curves and corresponding eye diagrams of the BTB OOK signal and the multicast channels. O: signal orthogonally polarized to probes. P: signal parallel polarized to probes. All the eye diagrams are measured when the SOP of the signal is orthogonally polarized to the probes.

Fig. 4 and Fig. 5 show the BER curves and the corresponding eye diagrams of the OOK and DPSK multicast channels. All the eye diagrams are measured when the SOP of the signal is orthogonally polarized to the probes.

When the SOP of the input signal is parallel to the probes, the maximum power penalties of the OOK and DPSK multicast channels are less than 0.7 dB and 0.8 dB at $\text{BER} = 10^{-9}$, compared to the back to back (BTB) input signal. However, the maximum power penalties of the OOK and DPSK multicast channels increase to 1.5 dB and 1.25 dB, when the SOP of the input signal is orthogonal to the probes.

The power penalty of Ch4 is around 0.2 dB for both OOK and DPSK signal when the SOP of the signal is orthogonally polarized to the probes. As the powers of Ch4 in Fig. 3 (a) and

(b) are almost same, it is expected that there will be little difference on the eye diagram and BER of Ch4 for the co-polarized case.

Table II summarizes the power penalty performance of the six FWM generated OOK and DPSK multicast channels when the signal is orthogonally (O) and parallel (P) to the probes. It can be seen that there is around up to 1 dB power penalty difference for the OOK multicast signals (see Ch3). While for the DPSK multicast signals, the power penalty difference is up to 0.75 dB (see Ch2). This extra 1 dB and 0.75 dB power penalty is due to the 5 dB lower CE, and more ASE noise is introduced by EDFA2.

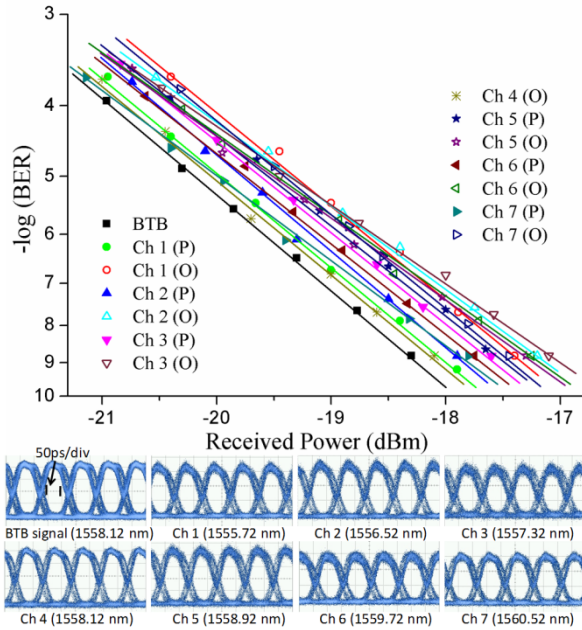


Fig. 5. BER curves and corresponding eye diagrams of the BTB DPSK signal and the multicast channels. O: signal orthogonally polarized to probes. P: signal parallel polarized to probes. All the eye diagrams are measured when the SOP of the signal is orthogonally polarized to the probes.

TABLE II
Power penalties of the six FWM generated OOK and DPSK multicast channels at BER = 10^{-9} when the signal is orthogonally (O) and parallel (P) to the probes.

	Power penalties of OOK signals (dB)		Power penalties of DPSK signals (dB)	
	P	O	P	O
Ch1	0.35	0.8	0.25	0.95
Ch2	0.7	1.25	0.4	1.15
Ch3	0.5	1.5	0.7	1.25
Ch5	0.4	1.1	0.8	1.05
Ch6	0.55	0.9	0.6	1.1
Ch7	0.3	0.6	0.5	0.85

By varying the SOP of the modulated signal, the residual 5 dB polarization fluctuation only results in around 1 dB and 0.75 dB power penalty difference to the OOK and DPSK multicast signals respectively. This difference in power penalty can be further reduced by using an EDFA with lower noise figure (NF).

B. Multicasting in SOA

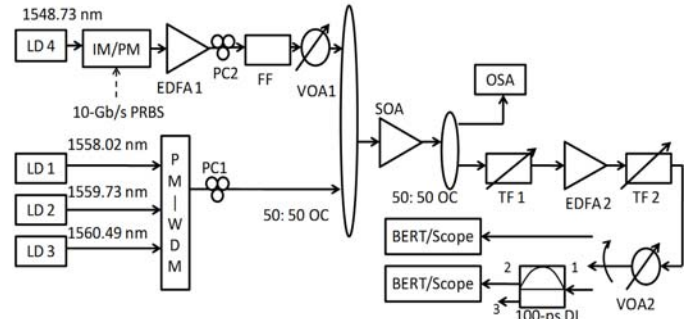


Fig. 6. Experimental setup. LD: laser diode. FF: fixed-wavelength filter. OSA: optical spectrum analyzer. IM: intensity modulator. PM: phase modulator. PC: polarization controller. SOA: semiconductor optical amplifier. OC: optical coupler. EDFA: erbium doped fiber amplifier. PRBS: pseudo-random bit sequence. PM-WDM: polarization maintaining wavelength division multiplexer. DI: delay interferometer. VOA: variable optical attenuator. TF: tunable-wavelength filter.

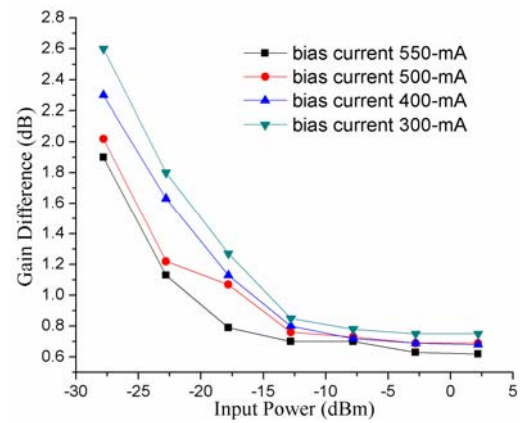


Fig. 7. The measured polarization dependent gain difference of the SOA. The bias current is set at 550-mA, 500-mA, 400-mA, and 300-mA respectively.

The SOA based multicasting experimental setup is shown by Fig. 6, which is similar to the experimental setup using the HNLf. LD1 (at 1558.02 nm), LD2 (at 1559.73 nm), and LD3 (at 1560.49 nm) work as three probes and their optical powers coupled into the SOA are set at 6.9-dBm, 3-dBm, and 4.1-dBm respectively. The wavelength of the signal is at 1548.73 nm and the power of the signal coupled to the SOA is set at 7-dBm by using the VOA1. PC1 and PC2 are used to adjust the SOPs of the co-polarized probes and signal.

The SOA (CIP-XN-OEC-1550) being used here has a small signal gain of around 34 dB, and a 16.5-dBm saturation output power when the bias current is set at 550-mA. The carrier recovery time of this SOA is typically 10-ps, which does not cause any degradation on the eye diagrams of the 10-Gbit/s data signal.

Fig. 7 shows the measured polarization dependent gain (PDG) difference of the SOA when the bias current is set at 550-mA, 500-mA, 400-mA, and 300-mA respectively. It can be seen that the gain difference becomes small when the power of input signal increases. The PDG difference is less than 1 dB when the power of input signal is above -12.5-dBm. While increasing the

bias current of the SOA, the PDG difference also decreases.

Fig. 8 shows the optical spectra at the output of the SOA when the SOPs of the three probes are fixed at a random chosen state. The bias current of the SOA is set at 550-mA. It can be seen that there are seven multicast channels individually located at 1546.26 nm (Ch1), 1547.02 nm (Ch2), 1547.97 nm (Ch3), 1548.73 nm (Ch4), 1549.49 nm (Ch5), 1550.44 nm (Ch6), and 1551.2 nm (Ch7). Because the CE of FWM arising in the SOA is much higher than that in the HNLf, some high order FWM idlers are also generated. Once we assign the probes with the same wavelength separations as the configuration using in the HNLf (0.8 nm between LD2 and LD3, 1.6 nm between LD1 and LD 2, and 2.4 nm between LD1 and LD3), some of the high order FWM idlers will overlap with the multicast channels and consequently introduce significant in-band crosstalk. The eye diagrams of these multicast channels are severely degraded and an error floor occurs at the BER of 10^{-4} . To avoid such crosstalk, we set the wavelengths of LD1 at 1558.02 nm, LD2 at 1559.73 nm, and LD3 at 1560.49 nm. Thus the crosstalk can be suppressed by using the TF2.

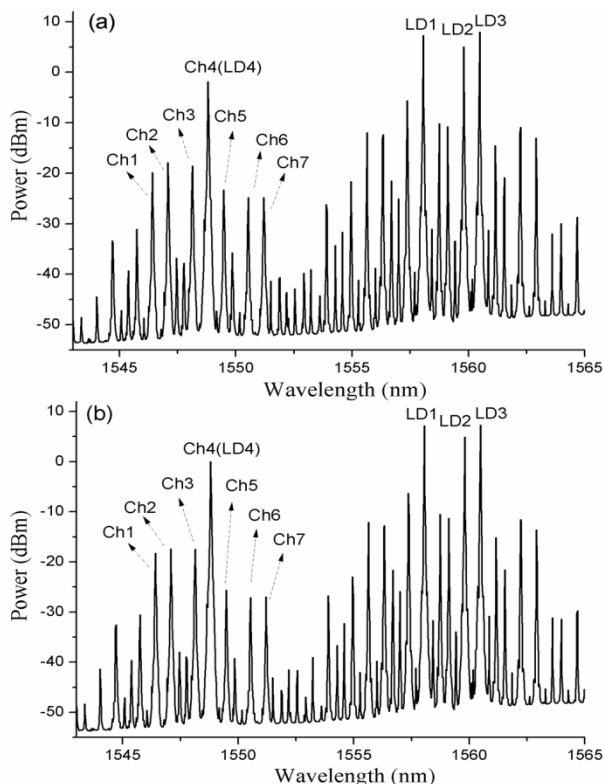


Fig. 8 (a) and (b). Optical spectra measured by the OSA when the OOK signal has minimum (a) and maximum (b) gain in the SOA due to the polarization dependent gain.

Due to the PDG in the SOA, Fig. 8 (a) shows the optical spectra measured by the OSA when the OOK signal has minimum gain in the SOA by adjusting PC2. While Fig. 8 (b) shows the optical spectra that the OOK signal has maximum gain in the SOA by adjusting PC2.

It can be seen that the PDG difference of the signal (Ch4) is around 2 dB. In addition, the conversion power of Ch1-Ch3 in Fig. 8 (a) is up to about 1.5 dB lower than that in Fig. 8 (b),

while the conversion power of Ch5-Ch7 in Fig. 8 (a) is up to around 2.5 dB higher than that in Fig. 8 (b). This shows that the polarization sensitivity has been reduced to within 2.5 dB in the SOA. Moreover, Ch2 and Ch6 have the largest and lowest conversion power in the obtained multicast channels, respectively. Their conversion power difference is 6.5 dB in Fig. 8 (a) and 9.5 dB in Fig. 8 (b). Compared with around 1 dB conversion power difference in the HNLf, this larger conversion power difference may be due to the PDG in the SOA, wavelength dependent gain in the SOA that leads to different gains for the probes, signal and the new multicast channels, and wavelength dependent relative conversion efficiency functions in the SOA.

Because the power conversion fluctuation in the SOA is less than 2.5 dB, we believe that the power penalty difference is much smaller than that in the HNLf. We measure all the eye diagrams and BER curves by setting both PC1 and PC2 in a fixed random state.

Fig. 9 shows the BER curves and the corresponding eye diagrams of the OOK modulated multicast channels. Compared with the BTB case, it can be seen that the largest power penalty of these multicast channels is less than 3.1 dB at $BER = 10^{-9}$.

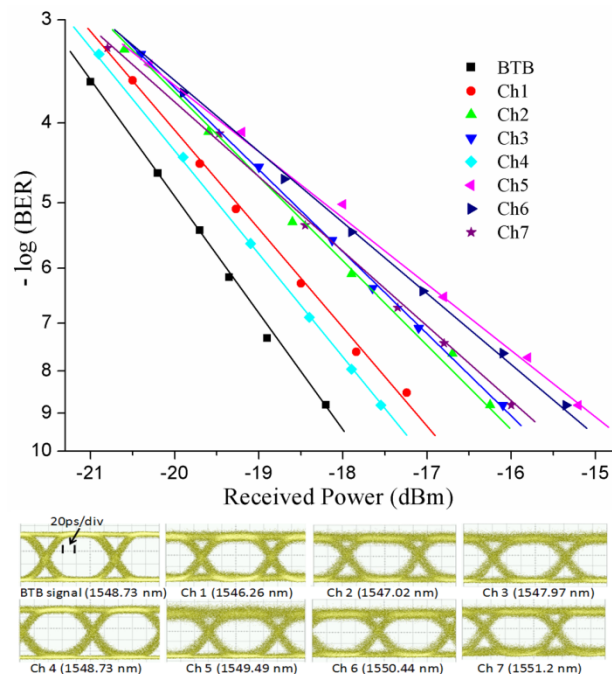


Fig. 9. BER curves and corresponding eye diagrams of the BTB OOK signal and the multicast channels.

The BER curves and the corresponding eye diagrams of the DPSK modulated multicast channels are illustrated by Fig. 10. And the maximum power penalty of these multicast channels is less than 1.1 dB.

According to Fig. 9 and Fig. 10, multicast channels Ch5-Ch7 have higher power penalties than those of Ch1-Ch3. This is because the former ones have lower conversion power than those of the later ones, and more ASE noise is introduced by EDFA2. And this difference in power penalty among different

multicast channels can be also further reduced by using an EDFA with lower NF. In addition, the reason why the OOK multicast signals have a higher power penalty than the DPSK signals is that the XGM effect in the SOA degrades the quality of the OOK multicast signals. This XGM effect is much less significant when multicasting the DPSK signal, owing to its constant envelope in the time domain.

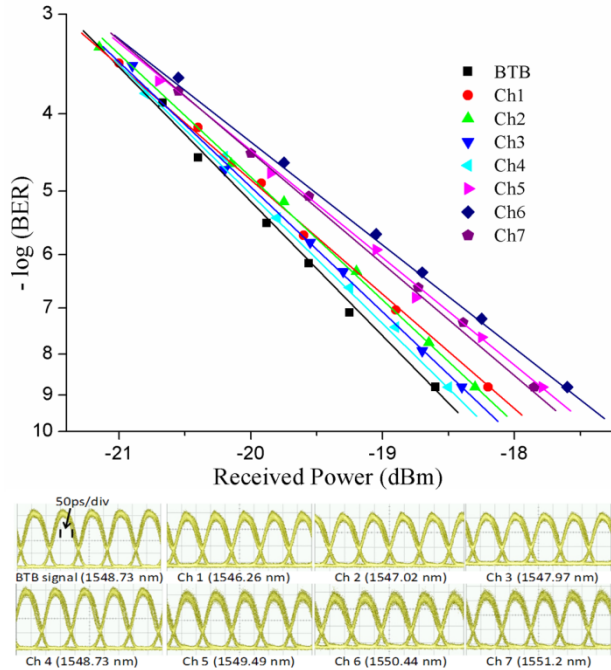


Fig. 10. BER curves and corresponding eye diagrams of the BTB DPSK signal and the multicast channels.

Fig. 11 gives the optical spectra at the output of the SOA when the bias current is set at 550-mA, 450-mA, 350-mA, and 250-mA, respectively. The input SOPs of the signal and the three probes are both set at a fixed random state. From Fig. 10, we can see that a higher bias current results in a higher gain and conversion power to the signal and the multicast channels. The gain and conversion power difference of the signal and multicast channels is within 5 dB and 10 dB when the bias current of the SOA is varying from 250-mA to 550-mA.

C. Discussions

The experimental results show that seven multicast channels can be obtained using either the HNLf or the SOA. Although the residual polarization sensitivity in the SOA is around 2.5 dB smaller than that in the HNLf, the power difference among the generated multicast channels is around 9.5 dB in the SOA, which is much higher than the 1 dB difference measured in the HNLf. Due to the high FWM CE in the SOA, another issue that needs to be addressed is the crosstalk generated from other high order FWM idlers when the SOA is used for multicasting. It is found that the BER error floor at 10^{-4} will occur if we assign the probes with the same wavelength separations as the same configuration using in the HNLf. However, this issue can be resolved by slightly detuning the wavelength separations of the

probes, e.g., setting LD1 at 1558.02 nm, LD2 at 1559.73 nm, and LD3 at 1560.49 nm.

Moreover, the maximum power penalty of the OOK multicast signals in the SOA is around 3.1 dB, which is about 1.6 dB higher than that in the HNLf. This is due to the XGM effect induced crosstalk in the SOA. Such a crosstalk can be suppressed when the phase modulated signals are multicasting, e.g., the maximum power penalty of the DPSK multicast signals is reduced to 1.1 dB in the SOA.

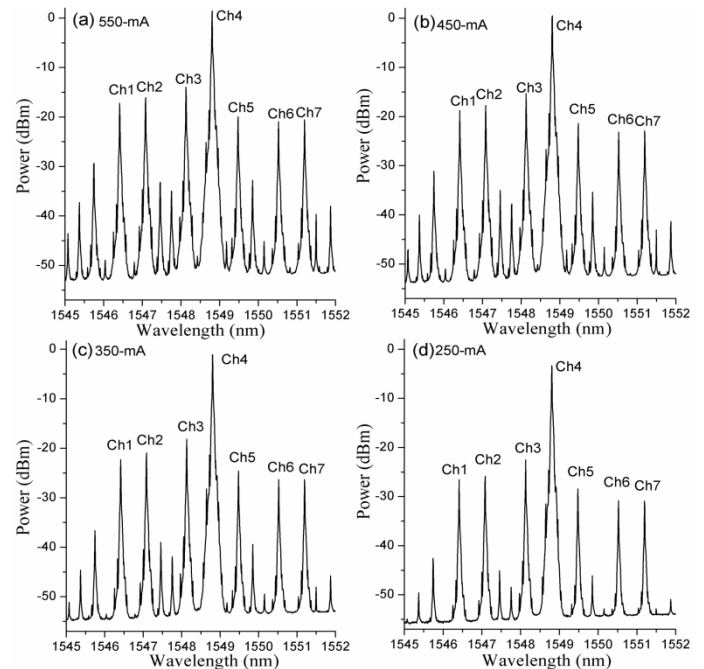


Fig. 11. Optical spectra at the output of the SOA when the bias current of the SOA is 550-mA (a), 450-mA (b), 350-mA (c), and 250-mA (d).

IV. CONCLUSION

In summary, we have proposed and experimentally demonstrated an all-optical modulation-format and bit-rate transparent wavelength multicast scheme based on the FWM effect in both an HNLf and an SOA. By using three co-polarized probes and a modulated signal, seven multicast channels are generated. Meanwhile the proposed multicast scheme can significantly reduce the polarization sensitivity from more than 20 dB to about 5 dB in the HNLf and 2.5 dB in the SOA. The low polarization sensitivity leads to a difference of less than 1 dB in the power penalty of the multicast channels. Comprehensive multicasting performance comparison of the OOK and DPSK signals in the HNLf and the SOA is reported. It is found that the converted power differences of the generated multicast channels in the SOA is around 9.5 dB, and this is much higher than the 1 dB difference measured in the HNLf. And this larger conversion power difference may be due to the PDG in the SOA, wavelength dependent gain in the SOA that leads to different gains for the probes, signal and the new multicast channels, and wavelength dependent relative conversion efficiency functions in the SOA. In addition, the maximum power penalties of the DPSK multicast channels in the HNLf and the SOA are less than 1.25 dB and 1.1 dB respectively. While the maximum power penalty of the OOK

multicast channels in the SOA is around 3.1 dB, which is 1.6 dB higher than that in the HNLFF. This is due to the XGM effect induced crosstalk. And such a crosstalk in the SOA can be suppressed when the phase modulated signals are used.

REFERENCES

- [1] M. J. O'Mahony, C. Politi, D. Klionidis, R. Nejabati, and D. Simeonidou, "Future optical network," *J. Lightw. Technol.*, vol. 24, no. 12, pp. 4684-4696, Dec. 2006.
- [2] S. J. Ben Yoo, "Optical packet and burst switching technologies for the future photonic internet," *J. Lightw. Technol.*, vol. 24, no. 12, pp. 4468-4492, Dec. 2006.
- [3] P. Gambini *et al.*, "Transparent optical packet switching: network architecture and demonstrators in the KEOPS project," *IEEE J. Select. Areas Commun.*, vol. 16, no. 7, pp. 1245-1259, Sep. 1998.
- [4] David K. Hunter *et al.*, "2x2 buffered switch fabric for traffic routing, merging, and shaping in photonics cell networks," *J. Lightw. Technol.*, vol. 15, no. 1, pp. 86-101, Jan. 1997.
- [5] S. Yao, B. Mukherjee, S. J. B. Yoo, and S. Dixit, "A unified study of contention-resolution in optical packet-switched network," *J. Lightw. Technol.*, vol. 21, no. 3, pp. 672-683, Mar. 2003.
- [6] C.-S. Chang, D.-S. Lee, and C.-Y. Yue, "Providing guaranteed rate services in the load balanced Brikhoff-von Neumann switches," *IEEE/ACM Trans. Networking*, vol. 14, no. 3, pp. 644-656, Jun. 2006.
- [7] B. Prabhakar, N. McKeown, and R. Ahuja, "Multicast scheduling for input-queued switches," *IEEE J. Select. Areas Commun.*, vol. 15, no. 5, pp. 855-866, Jun. 1997.
- [8] J. Gripp, J. E. Simsarian, J. D. LeGrange, P. Bernasconi, and D. T. Neilson, "Photonic terabit routers: the IRIS project," in *Proc. OFC/NFOEC2010*, San Diego, CA, Mar. 2010, Paper OThP3.
- [9] P. R. Prucnal, "Optically processed self-routing, synchronization, and contention resolution for 1-D and 2-D photonic switching architectures," *IEEE J. Quantum Electron.*, vol. 29, no. 2, pp. 600-612, Feb. 1993.
- [10] G. N. Rouskas, "Optical layer multicast: Rationale, building blocks, and challenges," *IEEE/ACM Trans. Network*, vol. 17, no. 1, pp. 60-65, Jan./Feb. 2003.
- [11] Y.-K. Yeo, J. Yu, and G.-K. Chang, "A broadcast and multicast-enabled switch architecture utilizing a gateless channel selection scheme," in *Proc. OFC/NFOEC2006*, Anaheim, CA, Mar. 2006, Paper OTuG7.
- [12] G.-K. Chang, J. Yu, Y.-K. Yeo, A. Chowdhury, and Z. Jia, "Enabling technologies for next-generation optical packet-switching networks," *Proc. of IEEE*, vol. 94, no. 5, pp. 892-910, May 2006.
- [13] A. M. J. Koonen *et al.*, "Label-controlled optical routing-technologies and applications," *IEEE J. Select. Topics Quantum Electron.*, vol. 13, no. 5, pp. 1540-1550, Sep./Oct. 2007.
- [14] D. Gurkan, S. Kumar, A. E. Willner, K. R. Parameswaran, and M. M. Fejer, "Simultaneous label swapping and wavelength conversion of multiple independent WDM channels in an all-optical MPLS network using PPLN waveguides as wavelength converters," *J. Lightw. Technol.*, vol. 21, no. 11, pp. 2739-2745, Nov. 2003.
- [15] Z. Xu, T.-H. Cheng, Y.-K. Yeo, Y. Wang, D. Wang, and J. Liu, "Simultaneous erasure and rewriting of a subcarrier-multiplexed label in an all-optical label swapping scheme," *Opt. Express*, vol. 18, no. 3, pp. 1974-1980, Jan. 2010.
- [16] Y.-K. Yeo, Z. Xu, D. Wang, J. Liu, Y. Wang, and T.-H. Cheng, "High-speed optical switch fabrics with large port count," *Opt. Express*, vol. 17, no. 13, pp. 10990-10997, Jun. 2009.
- [17] R. Langenhorst *et al.*, "Fiber loop optical buffer," *J. Lightw. Technol.*, vol. 14, no. 3, pp. 324-335, Mar. 1996.
- [18] S. Fu, P. Shum, L. Zhang, C. Wu, and A. M. Liu, "Design of a SOA-based dual-loop optical buffer with a 3x3 collinear coupler: guideline and optimization," *J. Lightw. Technol.*, vol. 24, no. 7, pp. 2768-2778, Jul. 2006.
- [19] R. S. Tucker, P.-C. Ku, and Constance J. C.-H., "Slow-light optical buffers: capabilities and fundamental limitations," *J. Lightw. Technol.*, vol. 23, no. 12, pp. 4046-4066, Dec. 2005.
- [20] J. Liu, T.-H. Cheng, Y.-K. Yeo, Y. Wang, L. Xue, W. Rong, L. Zhou, G. Xiao, D. Wang, and X. Yu, "Stimulate Brillouin scattering based on broadband tunable slow-light conversion in a highly nonlinear photonic crystal fiber," *J. Lightw. Technol.*, vol. 27, no. 10, pp. 1279-1285, May 2009.
- [21] O. Liboiron-Ladouceur, A. Shacham, B. A. Small, B. G. Lee, H. Wang, C. P. Lai, A. Bieberman, and K. Bergman, "The data Vortex optical packet switched interconnection Network," *J. Lightw. Technol.*, vol. 26, no. 13, pp. 1777-1789, Jul. 2008.
- [22] C. Bornholdt, J. Slovak, and B. Sartorius, "Semiconductor-based all-optical 3R regenerator demonstrated at 40 Gbit/s," *Electron. Lett.*, vol. 40, no. 3, pp. 192-194, Feb. 2004.
- [23] Y. Awaji, H. Furukawa, B. J. Puttnam, and N. Wada, "Burst-mode optical amplifier," in *Proc. OFC/NFOEC*, San Diego, CA, Mar. 2010, Paper OTh14.
- [24] Z. Pan, Z. Zhu, M. Funabashi, H. Yang, and S. J. B. Yoo, "101-hop cascaded operation of an optical-label switching router with all-optical clock recovery and 3R regeneration," *IEEE Photon. Technol. Lett.*, vol. 18, no. 15, pp. 1654-1656, Aug. 2006.
- [25] J. Yu, X. Zheng, F. Liu, C. Peucheret, Anders T. Clausen, Henrik N. Poulsen, and Palle Jeppesen, "8 x 40 Gb/s 55-km WDM transmission over conventional fiber using a new RZ optical source," *IEEE Photon. Technol. Lett.*, vol. 12, no. 3, pp. 912-914, Jul. 2000.
- [26] N. Yan, H.-D. Jung, I. T. Monroy, H. D. Waardt, and T. Koonen, "All-optical multi-wavelength conversion with negative power penalty by a commercial SOA-MZI for WDM wavelength multicast," in *Proc. OFC/NFOEC*, Anaheim, CA, Mar. 2007, Paper JWA36.
- [27] G. Contestabile, N. Calabretta, R. Proietti, and E. Ciaramella, "Double-stage cross-gain modulation in SOAs: An effective technique for WDM multicasting," *IEEE Photon. Technol. Lett.*, vol. 18, no. 1, pp. 181-183, Jan. 2006.
- [28] C. H. Kwok, S. H. Lee, K. K. Chow, C. Shu, C. Lin, and A. Bjarklev, "Polarization-insensitive all optical wavelength multicasting by self phase-modulation in a photonic-crystal fiber," in *Proc. CLEO2006*, Long Beach, CA, May 2006, Paper CTuD4.
- [29] L. Xu, N. Chi, K. Yvind, L. J. Christiansen, L. K. Oxenløwe, J. Mørk, P. Jeppesen, and J. Hanberg, "7x40 Gb/s base-rate RZ all-optical broadcasting utilizing an electroabsorption modulator," *Opt. Express*, vol. 12, no. 3, pp. 717-723, Feb. 2004.
- [30] K. K. Chow, and C. Shu, "All-optical signal regeneration with wavelength multicasting at 6x10 Gb/s using a single electro-absorption modulator," *Opt. Express*, vol. 12, no. 3, pp. 3050-3054, Jun. 2004.
- [31] K. K. Wong, G. W. Lu, K. C. Lau, P. K. A. Wai, and L. K. Chen, "All-optical wavelength conversion and multicasting by cross-gain modulation in a single-stage fiber optical parametric amplifier," in *Proc. OFC/NFOEC2007*, Anaheim, CA, Mar. 2007, Paper OTu14.
- [32] C.-S. Brès, N. Alic, E. Myslivets, and S. Radic, "Scalable multicasting in one-pump parametric amplifier," *J. Lightw. Technol.*, vol. 27, no. 3, pp. 356-363, Mar. 2009.
- [33] Mable P. Fok, and C. Shu, "Multipump four-wave mixing in a photonic crystal fiber for 6x10 Gb/s wavelength multicasting of DPSK signals," *IEEE Photon. Technol. Lett.*, vol. 19, no. 15, pp. 1166-1168, Aug. 2007.
- [34] G. W. Lu, K. S. Abedin, and T. Miyazaki, "DPSK multicast using multiple-pump FWM in Bismuths highly nonlinear fiber with high multicast efficiency," *Opt. Express*, vol. 16, no. 26, pp. 21964-21970, Dec. 2008.
- [35] D. Wang, T.-H. Cheng, Y.-K. Yeo, J. Liu, Z. Xu, Y. Wang, and G. Xiao, "All-optical modulation-transparent wavelength multicasting in a highly nonlinear fiber Sagnac loop mirror," *Opt. Express*, vol. 18, no. 10, pp. 10343-10353, May. 2010.
- [36] O. F. Yilmaz, S. R. Nuccio, X. Wang, J. Wang, I. Fazal, J.-Y. Yang, X. Wu, and A. E. Willner, "Experimental demonstration of 8-fold multicasting of a 100 Gb/s polarization-multiplexed OOK signal using highly nonlinear fiber," in *Proc. OFC/NFOEC2010*, San Diego, CA, Mar. 2010, Paper OWP8.
- [37] K. Lau, S. H. Wang, L. Xu, C. Lu, H. Y. Tam, and P. K. Wai, "All-optical multicast switch employing Raman-assisted FWM in dispersion-shifted fiber," *IEEE Photon. Technol. Lett.*, vol. 20, no. 20, pp. 1730-1732, Oct. 2008.
- [38] Y. Wang, C. Yu, T. Luo, L. Yan, Z. Pan, and A. E. Willner, "Tunable all-optical wavelength conversion and wavelength multicasting using orthogonally polarized fiber FWM," *J. Lightw. Technol.*, vol. 23, no. 10, pp. 3331-3338, Oct. 2005.
- [39] Y. Dai, and C. Shu, "Polarization-insensitive wavelength multicasting of RZ-DPSK Signal Based on four-wave mixing in a photonic crystal fiber with residual birefringence," in *Proc. OFC/NFOEC2010*, San Diego, CA, Mar. 2010, Paper OWP7.
- [40] D. Wang, T.-H. Cheng, Y.-K. Yeo, Y. Wang, Z. Xu, J. Liu, and G. Xiao, "Optical wavelength multicasting based on four wave mixing in highly nonlinear fiber with reduced polarization sensitivity," in *Proc. OFC/NFOEC2010*, San Diego, CA, Mar. 2010, Paper JWA47.

- [41] X. Zhou, and J. Yu, "Multi-level, multi-dimensional coding for high speed and high-spectral efficiency optical transmission," *J. Lightw. Technol.*, vol. 27, no. 16, pp. 3641-3653, Aug. 2009.
- [42] P. J. Winzer, and R. J. Essiambre, "Advanced optical modulation formats," *Proc. IEEE*, vol. 94, no. 5, pp. 952-985, May, 2006.
- [43] J. Ma, J. Yu, C. Yu, Z. Jia, X. Sang, Z. Zhou, T. Wang, and G. K. Chang, "Wavelength conversion based on four-wave mixing in high-nonlinear dispersion shifted fiber using a dual-pump configuration," *J. Lightw. Technol.*, vol. 24, no. 7, pp. 2851-2858, Jul. 2006.
- [44] J. P. R. Lacey, M. A. Summerfield, and S. J. Madden, "Tunability of polarization-insensitive wavelength converters based on four-wave mixing in semiconductor optical amplifier," *J. Lightw. Technol.*, vol. 16, no. 12, pp. 2419-2427, Dec. 1998.
- [45] G. Contestabile, L. Banchi, M. Presi, and E. Ciaramella, "Investigation of transparency of FWM in SOA to advanced modulation formats involving intensity, phase, and polarization multiplexing," *J. Lightw. Technol.*, vol. 27, no. 19, pp. 4256-4261, Oct. 2009.
- [46] T. Hasegawa, K. Inoue, and K. Oda, "Polarization independent frequency conversion by fiber four-wave mixing with a polarization diversity technique," *IEEE Photon. Technol. Lett.*, vol. 5, no. 8, pp. 947-949, Aug. 1993.
- [47] K. Inoue, "Polarization independent wavelength conversion using fiber four-wave mixing with two orthogonal pump lights of different frequencies," *IEEE Photon. Technol. Lett.*, vol. 12, no. 11, pp. 1916-1918, Nov. 1994.
- [48] K. K. Y. Wong, M. E. Marhic, K. Uesaka, and L. G. Kazovsky, "Polarization-Independent two-pump fibre optical parametric amplifier," *IEEE Photon. Technol. Lett.*, vol. 14, no. 7, pp. 911-913, Jul. 2002.
- [49] O. Aso, and S. Namiki, "Recent advances of ultra-broadband fiber optics wavelength converters," in *Proc. IEEE LEOS 2000 Annu. Meeting*, Nov. 13-16, 2000, vol. 2, pp. 683-684.
- [50] J. Zhou, N. Park, J. W. Dawson, K. J. Vahala, M. A. Newkirk, and B. I. Miller, "Efficiency of broadband four-wave mixing wavelength conversion using semiconductor traveling-wave amplifiers," *IEEE Photon. Technol. Lett.*, vol. 6, no. 1, pp. 50-52, Jan. 1994.